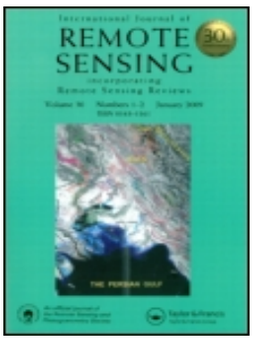

International Journal of Remote Sensing

ISSN: 0143-1161 (Print) 1366-5901 (Online) Journal homepage: https://www.tandfonline.com/loi/tres20

Lake water volume calculation with time series remote-sensing images

Shanlong Lu, Ninglei Ouyang, Bingfang Wu, Yongping Wei & Zelalem Tesemma

To cite this article: Shanlong Lu, Ninglei Ouyang, Bingfang Wu, Yongping Wei & Zelalem Tesemma (2013) Lake water volume calculation with time series remote-sensing images, International Journal of Remote Sensing, 34:22, 7962-7973, DOI: 10.1080/01431161.2013.827814

To link to this article: https://doi.org/10.1080/01431161.2013.827814

International Journal of Remote Sensing, 2013
Vol. 34, No. 22, 7962–7973, http://dx.doi.org/10.1080/01431161.2013.827814

Taylor & Francis
Taylor & Francis Group

Lake water volume calculation with time series remote-sensing images

Shanlong Lu[a]*, Ninglei Ouyang[a,b], Bingfang Wu[a], Yongping Wei[c], and Zelalem Tesemma[c]

[a]*State Key Laboratory of Remote Sensing Science, Institute of Remote Sensing and Digital Earth, Chinese Academy of Sciences, Beijing 100101, China;* [b]*School of Geosciences and Info-Physics, Central South University, Changsha 410083, China;* [c]*Melbourne School of Engineering, University of Melbourne, Parkville 3010 VIC, Australia*

(*Received 4 July 2012; accepted 6 July 2013*)

The volume of water in lakes is commonly estimated by combining data of water level variations with accurate bathymetry and shore topographic maps. However, bathymetry and shore topography data are often difficult to acquire, due to high costs for labour and equipment. This article presents an innovative method for calculating lake water volumes by using long-term time series remote-sensing data. Multi-spectral satellite remote-sensing images were used to map a lake's water surface area. The lake water surface boundaries for each year were combined with field-observed water levels to generate a description of the underwater terrain. The lake water volume was then calculated from the water surface area and the underwater terrain data using a constructed TIN (triangulated irregular network) volume model. Lake Baiyangdian, the largest shallow freshwater lake in the North China Plain, was chosen as the case study area. For the last 40 years the water levels of Lake Baiyangdian have reflected multiple dry and wet periods, which provide a good data series for the study of the proposed method. Archived Landsat MSS/TM/ETM+ and HJ-1A/B images from 1973 to 2011 were used as the basic data. The NDWI (normalized difference water index) and MNDWI (modified NDWI) were used to map the water surface of the lake, and the lake water volumes were calculated with the 3D Analyst tool of ArcMap 9.3. The results show that the estimated water volumes from remote-sensing images were very consistent with the volumes derived from the fitted equation of the lake storage capacity curve based on observed data.

1. Introduction

The water volume of a lake and its variations over time are fundamental properties because they affect the physical, chemical, and biological processes of lake ecosystems. The water area at a given site, or suite of sites, determines the vegetation structure and wildlife habitat, redoximorphic conditions and microbial activities, and organic matter concentrations, and therefore strongly influences the interactions of nutrients, pesticides, and other contaminants between lake sediments and its water column (Lane and D'Amico 2010). Water volumes in water bodies reflect the balance between rainfall and evaporation and interactions between surface and ground water systems (Brooks and Hayashi 2002; Medina et al. 2010). The volume of water bodies at particular times can be calculated by several methods depending on the availability of morphometric and areal data. The method most often

*Corresponding author. Email: lusl@irsa.ac.cn

adopted is to develop mathematical equations relating area and volume to depth and water level using morphometric data (Hayashi and van der Kamp 2000; Brooks and Hayashi 2002; Gamble et al. 2007; Gleason et al. 2007). Area (A), depth (h), and volume (V) relationships are usually determined from fine-resolution elevation maps based on detailed survey data (Hayashi and van der Kamp 2000). In these methods, a mathematical model is developed from an original underwater topographic map. Such models cannot reflect variations of the underwater terrain over time, so that as time passes the precision of simulations gradually decreases.

Another method is based on '3S' (RS, GPS, GIS) techniques. Wilcox and Huertos (2005) produced bathymetric surface maps of lake bottoms using a global positioning system receiver and laser transit survey data. Gleason et al. (2007) developed surface area-volume predictive models with field survey GPS data. Minke (2009) estimated time-effective water volumes at multiple spaces and scales by integrating the observed lowest and deepest water levels and a lidar (light detection and ranging) DEM (digital elevation model). Lane and D'Amico (2010) calculated the water volume of isolated wetlands in North Central Florida, USA, with lidar data and the triangulated irregular network (TIN) polygon volume model in ArcGIS. Although changes in underwater terrain and water volumes of lakes can be timely and accurately identified by these methods, they are often costly and it is labour intensive to obtain and process the original data (Flener et al. 2012; Furnans and Austin 2008).

It is easy to understand that a series of water surface boundaries of a lake at different water levels are similar to contour lines on a topographic map and can be used to reflect the underwater terrain of that lake, and that all lakes will experience wet–dry cycles, yearly or over multiple years. If information on the changes in area of the water surface of a lake at different times can be acquired, combined with field-observed water level data, the underwater terrain of the lake can be reconstructed (Feng et al. 2011). The development of satellite remote-sensing images over the last half century makes it possible to obtain information on the changes of water surface areas at different times (Wu and Lu 2011). In the last 20 years, multi-spectral remote-sensing images have been widely used for surface water monitoring, and many mapping methods have been proposed according to the characteristics of the water bodies' responsiveness to different spectral ranges. McFeeters (1996) developed the normalized difference water index (NDWI) to delineate open water bodies with reflective near-infrared radiation and visible green light. Xu (2006) improved the NDWI by using short-wave infrared radiation and renamed the index modified NDWI (MNDWI). Ouma and Tateishi (2006) proposed a water index (WI) for coastal boundary delineation by integrating the Tasseled Cap Wetness (TCW) index and the NDWI. In these methods, Landsat TM/ETM+ (Thematic Mapper/Enhanced Thematic Mapper Plus) (Lu et al. 2008; Zhang et al. 2011), MODIS (Moderate Resolution Imaging Spectroradiometer) (Rogers and Kearney 2004; Xiao et al. 2005), SPOT (Système Pour l'Observation de la Terre) (Bastawesy, Khalaf, and Arafat 2008), ASTER (Advanced Spaceborne Thermal Emission and Reflection Radiometer) (Sivanpillai and Miller 2010), and HJ-1A/B (Lu et al. 2011) satellite images have been widely used to map surface water.

This study presents an innovative method for lake water volume calculation that uses multi-spectral remote-sensing images of Landsat MSS/TM/ETM+ and HJ-1A/B (satellites launched in 2008 by the State Environmental Protection Administration and the National Committee for Disaster Reduction of China) to map water surface boundaries at different times; reconstructs the lake bottom terrain by integration of remotely sensed water surface boundaries and field-observed water levels; and calculates lake water volume at various time intervals. Our goal was to describe the method we developed to estimate

lake volume, apply it to Lake Baiyangdian, the largest lake in Northern China, and assess the method's accuracy for estimating lake volume in comparison to volumes calculated with the fitted empirical equation of the lake storage capacity curve.

2. Study area and data

The area of Lake Baiyangdian is about 366 km^2, and it is the largest shallow freshwater wetland in the North China Plain, located in Hebei Province at 38° 43′ N–39° 02′ N and 115° 38′ E–116° 07′ E (Figure 1). The region has a semiarid monsoon climate with average annual temperature of 12°C, average annual precipitation of 563.7 mm, and average annual pan evaporation of 1369 mm (Wang et al. 2010; Wang and Yang 2010).

Over the last 40 years, the high population density and rapid development of industry and agriculture in the North China Plain have resulted in water resource shortages (Xia 2002). Lake Baiyangdian has suffered from serious water depletion and has even dried out several times (Liu, Xie, and Huang 2006). At present, artificial supply of water to the lake plays a very important role in the maintenance of the lake's ecosystems. Artificial water deliveries were carried out 15 times from 1981 to 2003 (Yang, Chenand, and Yang 2010). The multiple dry–wet events and fluctuations in water levels in Lake Baiyangdian provide a good field site for the study of the proposed method.

In this study, because remote-sensing images with similar spatial resolution are the most important input data for lake bottom terrain reconstruction, Landsat MSS/TM/ETM+ and HJ-1A/B images were chosen as the major data sources. HJ-1A/B are sun-synchronous circular orbit satellites with an orbital altitude of 649 km. The single charge-coupled device (CCD) imagery width is 360 km, and the two satellites' constellation provides observation re-visit cycles every 48 hours. The CCD cameras have four bands – blue, green, red, and near-infrared spectrum – with a spatial resolution of 30 m and spectral range of

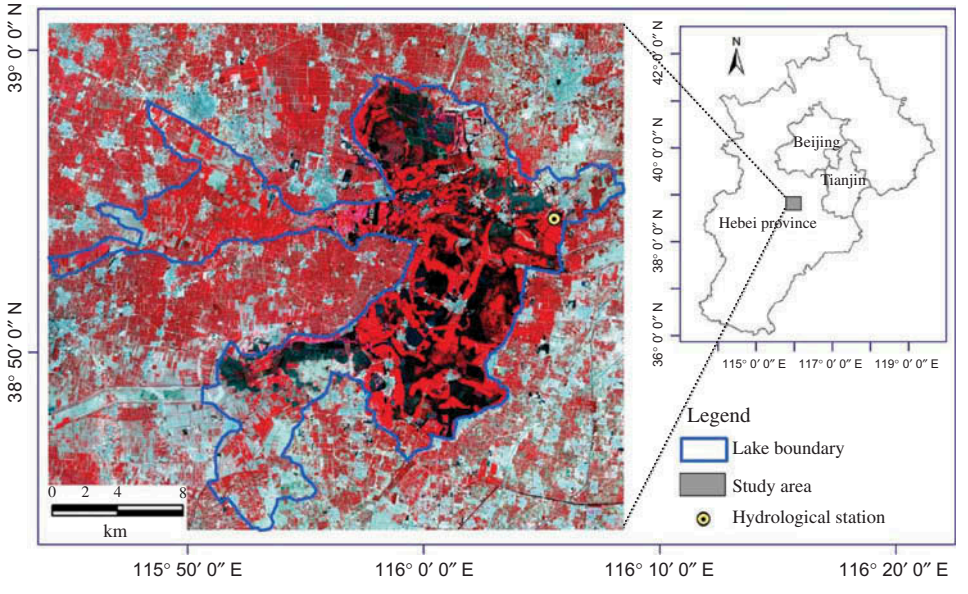

Figure 1. The study area of Lake Baiyangdian in the North China Plain (image acquired by Landsat TM on 8 June 2011).

0.43–0.9.0 μm. The two satellites have similar spectral range in the first four bands of the Landsat TM/ETM+ image. We downloaded all freely available Landsat MSS/TM/ETM+ images and HJ-1A/B from the US Geological Survey Earth Resources Observation and Science Center (EROS) and the China Centre for Resources Satellite Data and Application, respectively, and obtained 11 locally archived Landsat TM images from the Centre for Earth Observation and Digital Earth, Chinese Academy of Sciences. We obtained 58 phases of images in total. However, there were 30 phases of images acquired on dates for which there were no available water level data. On these dates the water levels were lower than the minimum detectable level of the Shifangyuan Hydrologic Station, or the lake was completely dried out. Consequently, we used only 28 images that were acquired on the dates where water level data were available (Figure 2). The details of acquisition times and spatial resolution of these images are given in Table 1. Because Landsat TM and ETM+ are

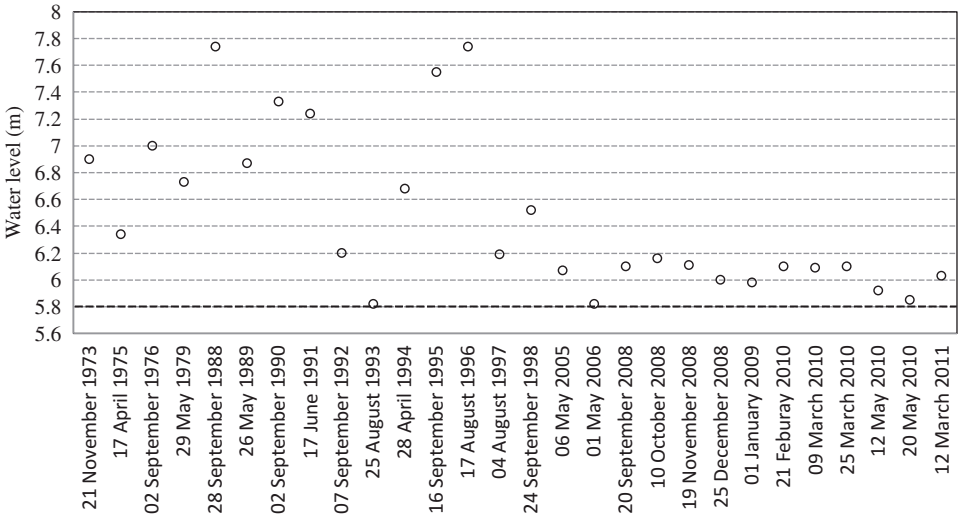

Figure 2. Water levels measured at Shifangyuan Hydrological Station at image acquisition. The thick dashed line shows the minimum level detectable level at this station.

Table 1. Remote-sensing data used in this article.

Data type	Acquisition time	Spatial resolution (m)
Landsat MSS	21 November 1973; 17 April 1975; 2 September 1976; 29 May 1979	57
Landsat TM	25 December 1988; 11 February 1989; 2 September 1990; 17 June 1991; 7 September 1992; 25 August 1993; 28 August 1994; 16 September 1995; 17 August 1996; 4 August 1997; 24 September 1998; 21 February 2010; 9 March 2010; 25 March 2010; 12 May 2010; 12 March 2011	30
Landsat ETM+	6 May 2005; 1 May 2006; 1 January 2009	30
HJ-1A/B	20 September 2008; 10 October 2008; 19 November 2008; 25 December 2008; 20 May 2010	30

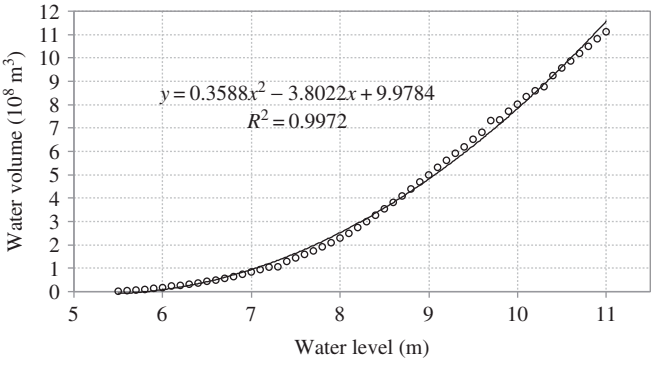

Figure 3. The fitted storage capacity curve of Lake Baiyangdian. 'y' denotes water volume and 'x' is water level.

fully matched, the images thus derived were geometrically corrected to the time-adjacent Landsat TM/ETM+ scenes. The root mean square errors (RMSEs) of the registration were controlled in one pixel.

The daily water levels were acquired from the Shifangyuan Hydrological Station at Lake Baiyangdian. The storage capacity curve (Figure 3) of the lake was fitted by using the annual average water level and volume data available from the Cangzhou Hydrographic Office, a division of the Haihe River Water Conservancy Committee, China (Li 2005). Annual water level and volume data are calculated using the field-observed daily water level and early field-observed underwater terrain data. The fitted equation of the storage capacity curve was used to calculate the lake volume at the date of image acquisition. The calculation result was used as the 'true' value to assess the volume estimated by the proposed method.

3. Methodology

The proposed method is composed of four steps – surface water mapping, water level contour creation, underwater topography modelling, and volume calculation (Figure 4). Percentage difference (PD), root mean square difference (RMSD), and linear regression are used as assessment methods.

3.1. Surface water mapping

Surface water mapping with multi-spectral remote-sensing images is based on the difference of the absorption and reflection of light between water and other features in different frequency bands. As reflections from water of the visible to infrared bands are gradually weakened, the surface water on an image can be delineated with the NDWI and MNDWI indices by the contrast of the visible wavelength with the near-infrared and short-wave infrared wavelengths (McFeeters 1996; Xu 2006). The NDWI and MNDWI indices were calculated with the following equations:

$$\mathrm{NDWI} = \frac{\rho_{\mathrm{Green}} - \rho_{\mathrm{NIR}}}{\rho_{\mathrm{Green}} + \rho_{\mathrm{NIR}}},\ \mathrm{MNDWI} = \frac{\rho_{\mathrm{Green}} - \rho_{\mathrm{SWIR}}}{\rho_{\mathrm{Green}} + \rho_{\mathrm{SWIR}}}, \tag{1}$$

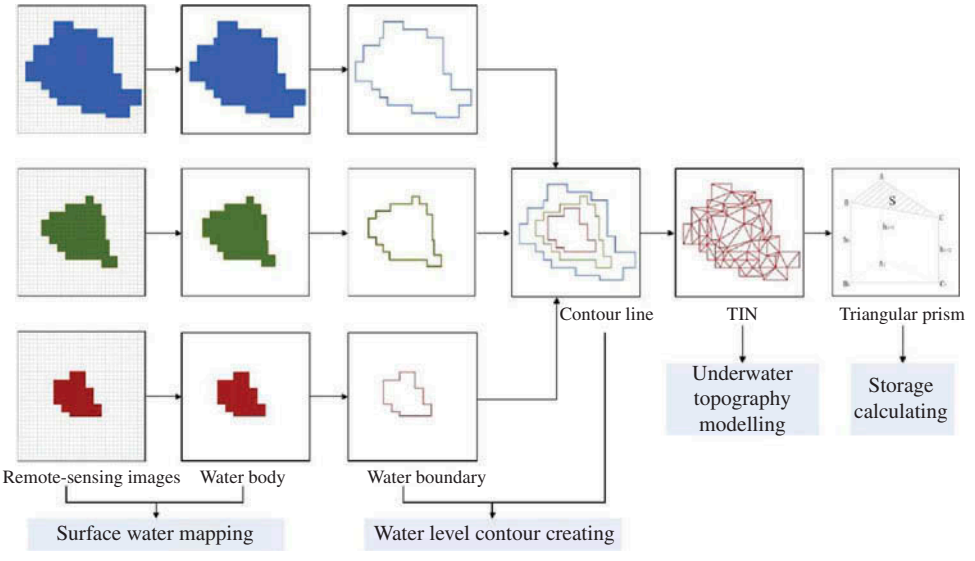

Figure 4. Conceptual framework of the lake water volume calculation method.

where ρ_{Green} is the green band, ρ_{NIR} is the near-infrared band of Landsat MSS and HJ-1A/B images, and ρ_{SWIR} is the short-wave infrared band of Landsat TM/ETM+ images.

Using NDWI and MNDWI, surface water was mapped on the 28 images taken at different times by extraction using the threshold segmentation method (Lu et al. 2012). Theoretically, the value of the water regions will be larger than 0 in the NDWI and MNDWI indices. However, due to vegetation influence, the extracted surface water regions obtained by threshold 0 are sometimes found to be smaller or larger than the actual regions. So, we manually set the segmentation threshold for each image through visual interpretation of the original images and the corresponding surface water indices. Eventually, the thresholds for the 28 images lay between –0.1 and 0.1.

3.2. *Water level contour creation*

Based on the surface water maps at different times, the vector boundary lines between water and the surrounding area were extracted with the Raster to Vector Tool in ArcMap 9.3. The water level contours were then created by assigning field-observed water level values to each line (Figure 5). Because we only have one water level datum for one time point, all water boundaries at each time point were set at the same water level value.

3.3. *Underwater topographic modelling*

Because the TIN model is superior to other split methods for topography simulation (Mi, Zai, and Jiang 2007), this was chosen to simulate underwater topography with all the vector water level contours. For the criss-crossing contours of the same water level at different times, a combination of these was used. Finally, the underwater terrain was modelled approximately as a set of non-overlapping triangles. Each triangle node has the coordinates x, y, and elevation value (depth of water), and each triangle surface has a certain slope angle. The number of triangles in different areas depends on the actual topography. In flat areas a relatively small number of triangles was generated, and vice versa.

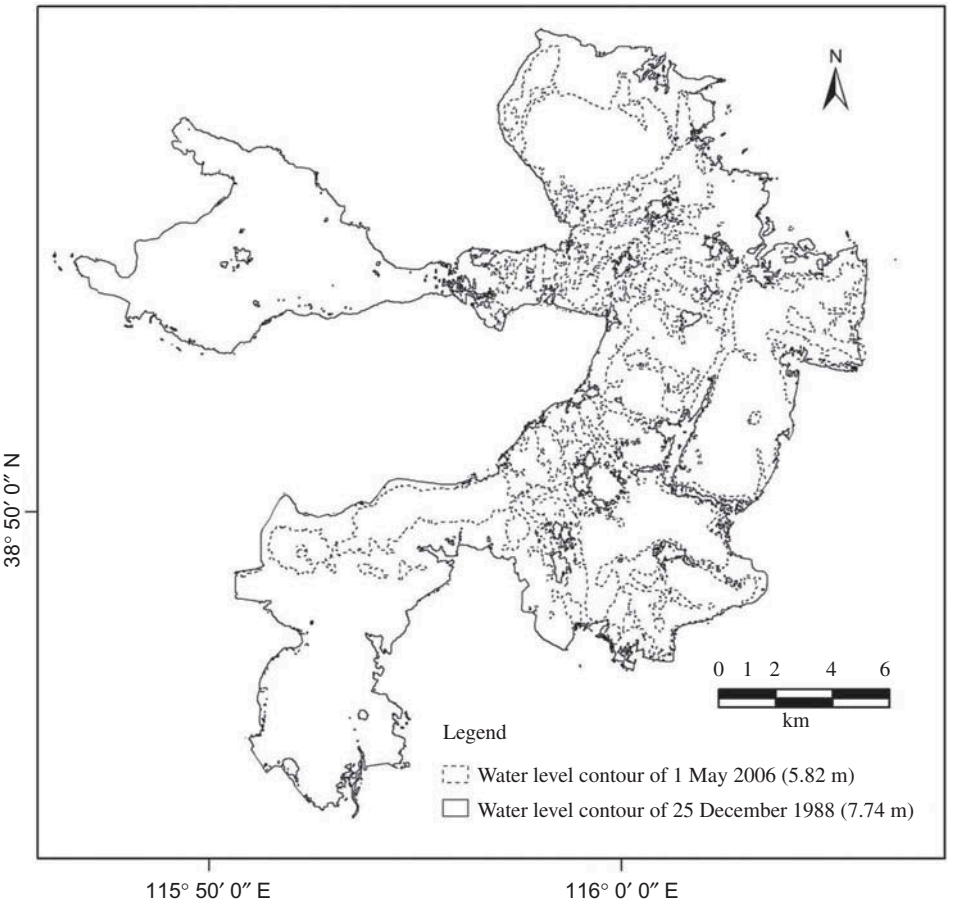

Figure 5. Lowest and highest water level contours created with the surface water maps. The region between the two contours is the dry–wet cycling zone. Being affected by lake level change, sometimes they are flooded, sometimes above water.

3.4. Volume calculation

The lake water volume was calculated with the Area and Volume Statistics module in ArcMap 9.3 3D Analyst, in which the physical model of the lake water body was formed with the intersection of the underwater terrain TIN and water surface. The physical model was divided into several triangular prisms by projecting each triangle vertex to the water surface. The water volume was then calculated by summing the volumes of each triangular prism (Mi, Zai, and Jiang 2007):

$$V = \sum_{i=1}^{n} S_i(h_i + h_{i+1} + h_{i+2})/3, \tag{2}$$

where V is the total volume (m^3), S_i is the projection area (m^2) of the underwater terrain triangle surface on the water surface, h_i, h_{i+1}, and h_{i+2} are distance (m) of the underwater triangle vertexes to the water surface, and n is the number of triangular grids (Lai, Fang, and Zhang 2009).

3.5. Assessment methods

The first assessment method of PD was calculated as follows:

$$\mathrm{PD} = \frac{(\text{Calculated Volume-True Volume})}{(\text{True Volume})}. \tag{3}$$

The second metric used was the RMSD:

$$\mathrm{RMSD} = \sqrt{\frac{\sum (\text{Calculated Volume-True Volume})^2}{N}}, \tag{4}$$

where N is the number of data compared.

Lastly, the linear regression (calculated vs true volume) was used to assess accuracy. As a measure of accuracy, the values obtained by the two methods would be in perfect agreement when regression has R^2 equal to one, a slope (β_1) equal to one, and an intercept (β_0) equal to zero.

4. Results and discussion

During the study period, the proposed method estimated volumes ranging from 0.6 to 208.1 million m^3, with a mean of 48.4 million m^3. The true volumes ranged from 0.3 to 204.4 million m^3 with a mean of 52.4 million m^3.

The mean PD and RMSD are somewhat low in comparison with the true volumes, with values of 11.2% and 9.3 million m^3, respectively. A two-tailed Student's t-test ($p = 0.81$) of the differences revealed no significant difference at the 5% level between the proposed method estimate and the true value. The linear regression analysis result also showed excellent estimation ability of the proposed method. R^2 and β_1 were very close to 1.0, with values of 0.9821 and 0.9677, respectively, whilst the intercept β_0 (–0.0235) was very close to zero (Figure 6).

In 1976, 1994, 1995, and 1996, the estimated water volumes were lower than those observed. The largest difference occurred in 1976 (Figure 7), possibly caused by wetland vegetation (reed) cover. Reeds are the major vegetation in Lake Baiyangdian and have the

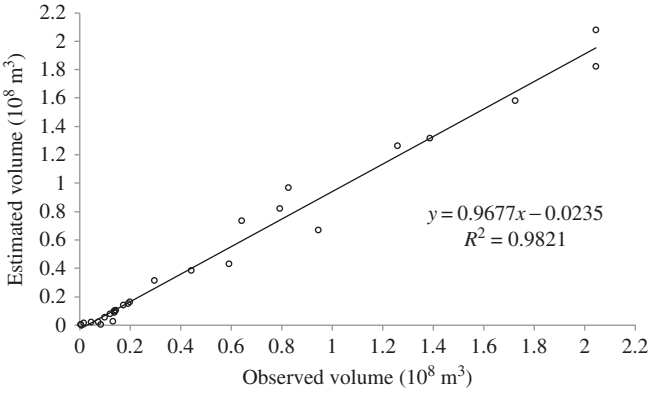

Figure 6. Comparison of linear regression for water volume between proposed (estimated) and true (observed) methods.

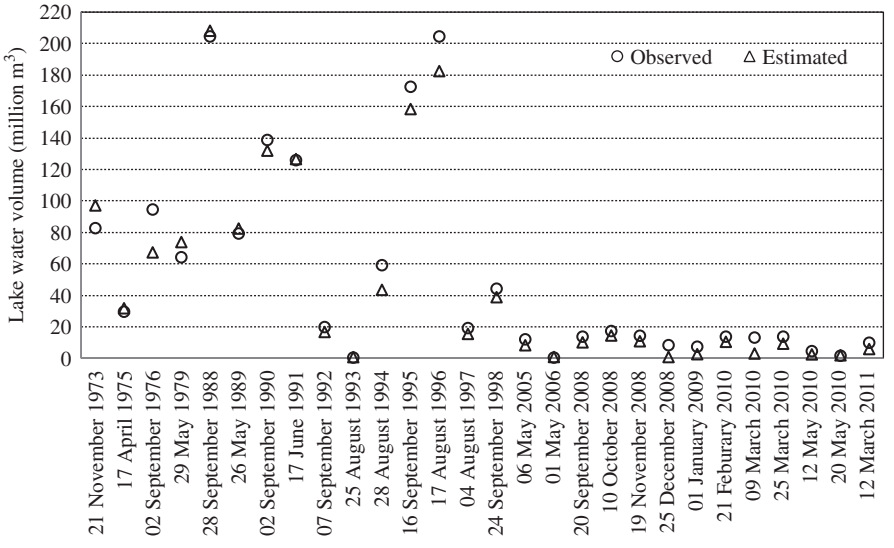

Figure 7. Comparison of volume between proposed (estimated) and true (observed) methods.

highest coverage during the months of August and September (Wang and Yang 2010). At this time of year, the water areas mapped by the multi-spectral remote-sensing images and lake water volumes would be underestimated. In 1973 and 1979, the estimated volumes were relatively larger than those observed (Figure 7), possibly caused by the water boundary data used for underwater topographic modelling. In the present study, the underwater terrain topography was reconstructed with all water boundaries mapped from the remote-sensing images. Changes in underwater terrain caused by human activities, mainly canal excavation for agricultural development during the most severe dry periods from 1983 to 1987 (BYDOL 2006; Liu, Xie, and Huang 2006), were incorporated into the reconstructed terrain TIN. So the estimated volumes before the dry period derived with the new terrain TIN may be higher than those observed.

Differences between the two methods at other times could be due to the different spatial resolutions of the multi-spectral satellite remote-sensing images, the accuracy of the field-measured water level, and the physical model employed. In this study, Landsat MSS/TM/ETM+ and HJ-1A/B images were used as the basic data for lake water mapping. However, the different spatial resolutions of Landsat MSS (57 m), Landsat TM/ETM+ (30 m), and HJ-1A/B (30 m) may cause areal mapping errors (Yao et al. 2012), and thus cause discrepancy in volume calculations. Generally, the water levels in different areas of a lake will show spatial gradients. If there were sufficient gauging stations to accurately portray the spatial gradients of surface water level, differences in water level in the same water boundaries should be considered in the step of the water level contour creation in this method. In this study, only Shifangyuan Hydrological Station water level data were used. The impact of water level spatial gradients could not be resolved. For the physical model characterization method, the triangular split method was used here but the use of trapezoid or square split methods would produce different results.

This proposed method has broad implications for water storage change monitoring in lakes with inter-annual or annual variations in water level, such as Poyang Lake (Cai and Ji 2009) and Dongting Lake (Ding and Li 2011) in China, the Areal Sea (Destouni, Asokan, and Jarsjo 2010) and Urmia Lake (Hassanzadeh, Zarghamiand, and Hassanzadeh 2012)

in Central Asia, Kivu Lake (Munyaneza et al. 2009) and Tana Lake (Dargahi and Setegn 2011) in Africa, and others. However, there are two factors that might affect such applications, the first being the availability of satellite remote-sensing images. A vast body of previous earth observation satellite data at moderate spatial resolution, such as multi-spectral data obtained from Landsat TM/ETM+, ASTER, Indian Remote Sensing satellite (IRS), China-Brazil Earth Resources Satellite (CBERS), and microwave data from ERS and Envisat, is available. However, due to differences in spatial resolution, spatial coverage, and data distribution policies, it is difficult to collect temporal and spatial data sets that are continuous and consistent. In this study, HJ-1A/B satellite data were successfully combined with Landsat MSS/TM/ETM+ serial data. On 11 February 2013, Landsat 8 of the Landsat Data Continuity Mission (LDCM) was launched, and it will continue to obtain valuable data as Landsat TM/ETM+ satellites have done in the past. In future, the temporally and spatially continuous and consistent data acquired by HJ-1A/B and Landsat 8 may improve application of the proposed method to other places. The second factor limiting application of the proposed method is the availability of field-observed water level data. The key step in this method is assigning water levels to each water boundary line in each year. Without field-measured water levels the underwater terrain cannot be constructed, and neither can the volume calculation be performed. This factor will limit the application of the method in ungauged lakes. In recent decades, ERS-1/2, ENVISAT, JASON-1, and TOPEX/POSEIDON(T/P) altimetry have been introduced to inland water level monitoring and have demonstrated high accuracy (Frappart et al. 2006; Medina et al. 2008; Munyaneza et al. 2009). The radar altimeter data provided by the Chinese HY-2 Satellite may have the same potential for application (http://www.nsoas.gov.cn/NewSite/Index.aspx). With such ancillary satellite data, the second limitation ought to be resolved.

5. Conclusions

We took advantage of yearly and multiple-year wet–dry cycle variations in lake water levels and used archived multi-spectral satellite remote-sensing images to develop an innovative approach to lake water volume calculation, using Lake Baiyangdian as a case study area. Good agreement between the proposed method's estimates of volumes and observed volumes in Lake Baiyangdian show that multi-spectral remote-sensing images, combined with observed water levels, is very useful for determining changes in lake water volumes over time. The obvious merit of this method as compared to the commonly used observational approach is that it can obtain temporal and spatial changes in lake bottom topography at much lower labour and data-processing cost.

In summary, the proposed water volume calculation method is useful for monitoring changes in inland lake water volume, especially for lakes with no underwater terrain data. At present there are no long-term temporal and spatial continuous satellite data or observed data, so integrative use of these two types of data is the best option. Our subsequent study will focus on the use of the multi-spectral and microwave remote-sensing images, radar altimeter data, and field-observation data in an integrated way to monitor inland lake water volumes.

Acknowledgements

This study was funded by the National Natural Science Foundation of China (No. 41101401 and No. 91025007) and the Non-profit Research Programme of the Ministry of Water Resource (No. 201101015). We are grateful to the US Geological Survey Earth Resources Observation and

Science Center (EROS), the Centre for Earth Observation and Digital Earth, Chinese Academy of Sciences, and the China Centre for Resources Satellite Data and Application for providing the Landsat MSS/TM/ETM+ and HJ-1A/B images. We are profoundly grateful to Professor Ian Willett from the University of Melbourne for carefully reviewing the article and providing valuable advice.

References

Bastawesy, M. A., F. I. Khalaf, and S. M. Arafat. 2008. "The Use of Remote Sensing and GIS for the Estimation of Water Loss from Tushka Lakes, Southwestern Desert, Egypt." *Journal of African Earth Sciences* 52: 73–80.

Brooks, R. T., and M. Hayashi. 2002. "Depth-Area-Volume and Hydroperiod Relationships of Ephemeral (Vernal) Forest Pools in Southern New England." *Wetlands* 22: 247–255.

BYDOL. 2006. "Baiyangdian Online." Assessed March 26, 2012. http://www.bydonline.cn/news-016fenxi.html

Cai, X., and W. Ji. 2009. "Wetland Hydrologic Application of Satellite Altimetry – A Case Study in the Poyang Lake Watershed." *Progress in Natural Science* 19: 1781–1787.

Dargahi, B., and S. G. Setegn. 2011. "Combined 3D Hydrodynamic and Watershed Modelling of Lake Tana, Ethiopia." *Journal of Hydrology* 398: 44–64.

Destouni, G., S. M. Asokan, and J. Jarsjo. 2010. "Inland Hydro-Climatic Interaction: Effects of Human Water Use on Regional Climate." *Geophysical Research Letters* 37: L18402. doi:10.1029/2010GL044153.

Ding, X., and X. Li. 2011. "Monitoring of the Water-Area Variations of Lake Dongting in China with ENVISATASAR Images." *International Journal of Applied Earth Observation and Geoinformation* 13: 894–901.

Feng, L., C. Hu, X. Chen, R. Li, L. Tian, and B. Much. 2011. "MODIS Observations of the Bottom Topography and Its Inter-Annual Variability of Poyang Lake." *Remote Sensing of Environment* 115: 2729–2741.

Flener, C., E. Lotsari, P. Alho, and J. Kǎayhkǒ. 2012. "Comparison of Empirical and Theoretical Remote Sensing Based Bathymetry Models in River Environments." *River Research and Applications* 28: 118–113.

Frappart, F., S. Calmant, M. Aauhope, F. Seyler, and A. Cazenave. 2006. "Preliminary Results of ENVISAT RA-2-Derived Water Levels Validation over the Amazon Basin." *Remote Sensing of Environment* 100: 252–264.

Furnans, J., and B. Austin. 2008. "Hydrographic Survey Methods for Determining Reservoir Volume." *Environmental Modeling & Software* 23: 139–146.

Gamble, D., E. Grody, J. Undercoffer, J. J. Mack, and M. Micacchion. 2007. *An Ecological and Functional Assessment of Urban Wetlands in Central Ohio*. Volume 2: Morphometric Surveys, Depth-Area-Volume Relationships and Flood Storage Function of Urban Wetlands in Central Ohio. Ohio EPA Technical Report WET/2007-3B, Ohio Environmental Protection Agency, Columbus, OH.

Gleason, R. A., B. A. Tangen, M. K. Laubhan, K. E. Kermesand, and J. N. H. Euliss. 2007. *Estimating Water Storage Capacity of Existing and Potentially Restorable Wetland Depressions in a Subbasin of the Red River of the North*. U.S. Geological Survey Open File Report 2007–1159. U.S. Geological Survey, Reston, VA.

Hassanzadeh, E., M. Zarghamiand, and Y. Hassanzadeh. 2012. "Determining the Main Factors in Declining the Urmia Lake Level by Using System Dynamics Modeling." *Water Resource Management* 26: 129–145.

Hayashi, M., and G. van der Kamp. 2000. "Simple Equations to Represent the Volume-Area-Depth Relations of Shallow Wetlands in Small Topographic Depressions." *Journal of Hydrology* 237: 74–85.

Lai, L., J. Fang, and Y. Zhang. 2009. "Reservoir Storage Capacity Calculation Using DEM Model." *Jiangxi Surveying and Mapping* 77: 41–43 (in Chinese).

Lane, C. R., and E. D'Amico. 2010. "Calculating the Ecosystem Service of Water Storage in Isolated Wetlands Using LiDAR in North Central Florida, USA." *Wetlands* 30: 967–977.

Li, J. 2005. "Study on Water Environment Safety Evaluation of Baiyangdian Lake Wetland." Master diss., HeBei Agricultural College (in Chinese).

Liu, C., G. Xie, and H. Huang. 2006. "Shrinking and Drying up of Baiyangdian Lake Wetland: A Natural or Human Cause?" *Chinese Geographical Science* 16: 314–319.

Lu, S., X. Shen, L. Zou, C. Li, Y. Mao, G. Zhang, W. Wu, Y. Liu, and Z. Zhang. 2008. "An Integrated Classification Method for Thematic Mapper Imagery of Plain and Highland Terrains." *Journal of Zhejiang University Science A* 9: 858–866.

Lu, S., B. Wu, H. Wang, N. Ouyang, and S. Guo. 2012. "Hydro-Ecological Impact of Water Conservancy Projects in the Haihe River Basin." *Acta Oecologica* 44: 67–74.

Lu, S., B. Wu, N. Yan, and H. Wang. 2011. "Water Body Mapping Method with HJ-1A/B Satellite Imagery." *International Journal of Applied Earth Observation and Geoinformation* 13: 428–434.

McFeeters, S. K. 1996. "The Use of Normalized Difference Water Index (NDWI) in the Delineation of Open Water Features." *International Journal of Remote Sensing* 17: 1425–1432.

Medina, C. E., J. Gomez-Enri, J. J. Alonso, and P. Villares. 2008. "Water Level Flucuations Derived from ENVISAT Radar Altimeter (RA-2) and In-Situ Measurements in a Subtropical Waterbody: Lake Izabal (Guatemala)." *Remote Sensing of Environment* 112: 3604–3617.

Medina, C. E., J. Gomez-Enri, J. J. Alonso, and P. Villares. 2010. "Water Volume Variations in Lake Izabal (Guatemala) from In Situ Measurements and ENVISAT Radar Altimeter (RA-2) and Advanced Synthetic Aperture Radar (ASAR) Data Products." *Journal of Hydrology* 382: 34–48.

Mi, H., J. Zai, and X. Jiang. 2007. "Contrast and Analysis of Reservoir Storage Calculation Methods." *Surveying and Mapping of Geology and Mineral Resources* 23: 1–4 (in Chinese).

Minke, A. G. N. 2009. "Estimating Water Storage of Prairie Pothole Wetlands." Master thesis, University of Saskatchewan, Saskatoon.

Munyaneza, O., U. G. Wali, S. Uhlenbrook, S. Maske, and M. J. Mlotha. 2009. "Water Level Monitoring Using Radar Remote Sensing Data: Application to Lake Kivu, Central Africa." *Physics and Chemistry of the Earth* 34: 722–728.

Ouma, Y. O., and R. Tateishi. 2006. "A Water Index for Rapid Mapping of Shoreline Changes of Five East African Rift Valley Lakes: An Empirical Analysis Using Landsat TM and ETM+ Data." *International Journal of Remote Sensing* 27: 3153–3181.

Rogers, A. S., and M. S. Kearney. 2004. "Reducing Signature Variability in Unmixing Coastal Marsh Thematic Mapper Scenes Using Spectral Indices." *International Journal of Remote Sensing* 25: 2317–2335.

Sivanpillai, R., and S. N. Miller. 2010. "Improvements in Mapping Water Bodies Using ASTER Data." *Ecological Informatics* 5: 73–78.

Wang, J., S. Lu, B. Wu, N. Yanand, and L. Pei. 2010. "The Study of Land Cover Change in Baiyangdian Wetland." *Geo-Information Science* 12: 1–9 (in Chinese).

Wang, Q., and Z. Yang. 2010. "Seasonal Environmental-Flow Demand Calculation of Reed Community (Phragmites Australis Var. Baiyangdiasis) Under Different Meteorological Conditions in Baiyangdian Lake China." *Procedia Environmental Sciences* 2: 1857–1864.

Wilcox, C., and M. L. Huertos. 2005. "A Simple, Rapid Method for Mapping Bathymetry of Small Wetland Basins." *Journal of Hydrology* 301: 29–36.

Wu, B., and S. Lu. 2011. "Watershed Remote Sensing: Methodology and a Paradigm in Hai Baisn." *Journal of Remote Sensing* 15: 201–223.

Xia, J. 2002. "Water Cycle and Water Resources Safety in North China: Problems and Challenges." *Haihe Water Resources* 21: 517–526 (in Chinese).

Xiao, X., S. Boles, J. Liu, D. Zhuang, S. Frolking, C. Li, W. Salas, and B. Moore III. 2005. "Mapping Paddy Rice Agriculture in Southern China Using Multi-Temporal MODIS Images." *Remote Sensing of Environment* 95: 480–492.

Xu, H. 2006. "Modification of Normalized Difference Water Index (NDWI) to Enhance Open Water Features in Remotely Sensed Imagery." *International Journal of Remote Sensing* 27: 3025–3033.

Yang, Y., H. Chenand, and Z. Yang. 2010. "Assessing Changes of Trophic Interactions during Once Anthropogenic Water Supplement in Baiyangdian Lake." *International Society for Environmental Information Sciences Annual Conference (ISEIS), Procedia Environmental Sciences* 2: 1169–1179.

Yao, X., S. Liu, M. Sun, J. Wei, and W. Guo. 2012. "Volume Calculation and Analysis of the Changes in Moraine-Dammed Lakes in the North Himalaya: A Case Study of Longbasaba Lake." *Journal of Glaciology* 58: 753–760.

Zhang, B., Y. Wu, L. Zhu, J. Wang, J. Li, and D. Chen. 2011. "Estimation and Trend Detection of Water Storage at Nam Co Lake, Central Tibetan Plateau." *Journal of Hydrology* 405: 161–170.